JOURNAL OF MATERIALS SCIENCE 22 (1987) 394–402

Effect of composition and grain size on slow plastic flow properties of NiAl between 1200 and 1400 K

J. DANIEL WHITTENBERGER
NASA-Lewis Research Center, Cleveland, Ohio 44135, USA

A series of ~15 μm diameter, polycrystalline B2 crystal structure NiAl alloys ranging in composition from 43.9 to 52.7 Al (at%) have been compression tested at constant velocities in air between 1200 and 1400 K. All materials were fabricated via powder metallurgy techniques with hot extrustion as the densification process. Seven intermediate compositions were produced by blending various amounts of two master heats of prealloyed powder; in addition a tenth alloy of identical composition, 48.25 Al, as one of the blended materials was produced from a third master heat. Comparison of the flow stress–strain rate behaviour for the two 48.25 Al alloys revealed that their properties were identical. The creep strength of materials for Al/Ni $\leqslant$ 1.03 was essentially equal, and deformation could be described by a single stress exponent and activation energy. Creep at low temperatures and faster strain rates is independent of grain sizes and appears to be controlled by a subgrain mechanism. However, at higher temperatures and slower strain rates, diffusional creep seems to contribute to the overall deformation rate.

1. Introduction

Of the B2 crystal structure binary aluminides under consideration for elevated temperature stuctural purposes, most attention has been focused on NiAl. Between 1960 and 1973 the elevated temperature mechanical behaviour of this intermetallic compound was extensively studied [1–11] both in tension and compression as functions of strain rate, composition and form (single crystals and polycrystals). Examination of these efforts reveals that some confusion over the role of composition and grain size on elevated temperature strength exists.

Grala [1] reported that the 1088 K tensile strength of NiAl generally decreases with increasing aluminium level in the range from 42 to 51.7 Al (all compositions in at% unless otherwise noted). In addition he noted that the 1088 K tensile strength of a Ni–42 Al alloy was decreased by a prior heat treatment which increased the grain size (no quantative data were given). As a follow-up to this observation he alloyed stoichiometic NiAl with 0.2, 0.45 and 0.9% Mo which decreased the grain sizes in comparison to unalloyed material. Results of 1088 and 1200 K tensile tests and a 1088 K stress rupture test indicated that the strength of the ternary intermetallics was improved over that of the larger grain-diameter binary material; however, the specific effect of grain size could not be separated from the influence of solid solution hardening and second-phase formation.

Lautenschlager *et al.* [2] studied the effects of composition and grain size on compressive stress–strain behaviour of binary NiAl alloys between 973 and 1173 K. Over the compressive strain-rate range from 5×10^{-3} to 5×10^{-5} sec^{-1}, they found for each composition that the strength of fine grain size (~200 μm) materials was equal to or greater than that of the coarse grain diameter (~1000 μm) ones. With respect to chemistry it was noted that deviations from stoichiometry increased strength; however, such behaviour was not continuous as strengths peaked at ~52 and ~42 Al with the hypostoichiometric material being the strongest.

At temperatures exceeding 900 K, Ball and Smallman [4] showed for a narrow composition range (47.9 to 51.1 Al) that the initial flow stress of polycrystalline (grain size not reported but greater than 100 μm), near stoichiometic NiAl is greatest. On the other hand, Pascoe and Newey [6] found that for 50 μm grain size materials, the 0.2% proof stress of Ni–48.9 Al was considerably less that that of either Ni–43 Al or Ni–53 Al. Rozner and Wasilewski [3] have also presented tensile data which reveal that a presumably small grain size, nominally stoichiometric NiAl is as strong, or stronger, than Ball and Smallman's or Pascoe and Newey's nominally Ni–50 Al materials for temperatures exceeding 1000 K. (The belief that Rozner and Wasilewski's intermetallic compound possessed a small grain size is based on the use of hot extrusion for fabrication and their report of some room temperature tensile ductility. This is the only known open literature citation of low-temperature tensile ductility in NiAl and would require a very small grain size according to current thinking [12].)

Two studies of the behaviour of polycrystalline NiAl in the near creep and creep regimes have also been undertaken. Vandervoort *et al.* [5]

0022–2461/87 $03.00 + .12

determined the flow stress–strain rate behaviour of Ni–44 Al (grain size ~ 600 μm), Ni–50.4 Al (grain size ~ 1000 μm) and Ni–54 Al (grain size ~ 600 μm) between 1073 and 1673 K and the compressive strain rate range from 10^{-3} to 10^{-5} sec^{-1}. They found that the flow stress for the near stoichiometric aluminide was least at the lower temperatures, but this composition became strongest at 1523 K. Yang and Dodd [8] examined steady state compressive creep between 973 and 1318 K of a series of six intermetallic compounds from 45 to 54 Al with the stoichiometric material having an approximately 450 μm grain size and the other alloys possessing ~ 200 to 250 μm grain diameters. At 1073 K, Ni–49 Al was weakest; however, as the test temperature increased, three groups of relative strength appeared where the extreme hypostoichiometric composition was strongest, the extreme hyperstoichiometric was weakest, and all the other compositions had about the same intermediate strength. Comparison of the behaviour for these two studies over similar temperatures, compositions and stain rates reveals that Vandervoort *et al.*'s materials are much weaker than those of Yang and Dodd, possibly due to the difference in microstructure.

Because of the uncertainty over composition and grain size effects in NiAl and the Lewis Research Center's interest in developing new elevated temperature structural materials for long-term application under severe conditions, a study of the influence of composition on the flow strength of a series of small, approximately equal grain-sized NiAl alloys was undertaken. Ten compositions ranging from 43.9 to 52.7 Al were produced by hot extrusion of blended, prealloyed powders and were tested in compression between 1200 and 1400 K in air at strain rates from about 10^{-4} to 10^{-7} sec^{-1}. Standard materiallographic procedures were used to characterize the materials prior to and after testing, and the usual temperature compensated-power law equations were utilized to evaluate flow stress–strain rate data. This work is one part of an overall effort to understand the mechanical behaviour of simple binary B2 aluminides.

2. Experimental procedure

Owing to the experience and capabilities of the Lewis Research Center, all intermetallic materials investigated in this study were produced via powder metallurgy techniques. Two master heats of prealloyed −80 mesh gas atomized NiAl powder were procured from Alloy Metals, Troy, Michigan, where one heat contained 52.7 Al and the other 43.9 Al. Based on their certified compositions seven intermediate aluminium levels were chosen around stoichiometry. Alloys suitable for testing were then produced by blending appropriate amounts of each heat in a Vee blender, vacuum encapsulating the mixed powders in 51 mm diameter, 6.4 mm thick wall steel extrusion cans, and extruding these at 1420 K and a nominally 16:1 reduction ratio.

An additional tenth alloy was prepared by a somewhat different procedure involving a 76 mm diameter, 6.4 mm thick wall steel can filled with prealloyed Ni–48.25 Al, −320 mesh powder. This billet was initially hot compacted at 1505 K and 1310 MPa for 10 sec, remachined to diameter, and then hot extruded at 1505 K and a 16:1 reduction ratio. Chemical analysis of selected as-extruded materials revealed that their composition was identical to the powder blends; chemistry of all the materials is given in Table I. All alloys contained ~ 0.2% interstitials and oxygen which originated from the master alloys.

TABLE I Chemistry and grain size of as-extruded NiAl intermetallic materials

Al (at %)	Al/Ni	Grain size (μm)
52.7*	1.118	15
51.6	1.070	15
50.6	1.028	16
49.91	1.00	13
49.2	0.972	17
48.25	0.932	14
47.0	0.889	18
45.5	0.837	16
43.9†	0.786	15
48.25‡	0.933	18

*Master alloy containing 0.01C, 0.05H, 0.004N and 0.14O.
†Master alloy containing 0.011C, 0.02H, 0.004N and 0.09O.
‡Master alloy containing 0.003C and 0.07O, alloy compacted and extruded from 76 mm tooling.

Cylindrical test specimens 5 mm diameter and 10 to 13 mm long were prepared by electrodischarge machining cores parallel to the extrusion direction from the as-extruded bars and grinding the cores to diameter and length. Elevated temperature mechanical properties were determined by constant velocity compression testing in air at crosshead speeds ranging from 2.12×10^{-2} to 2.12×10^{-6} mm sec^{-1} between 1100 and 1400 K. True compressive strains, stresses and strain rates were calculated from the autographically recorded load–time curves with assumptions of uniform deformation and conservation of volume. In general tests at the higher velocities were conducted to 20% or more deformation while the slower tests were terminated usually after 10% strain. Additional discussion of the specimen preparation and compression testing was published previously [13, 14].

The structure of as-extruded intermetallics and selected test coupons was examined by optical materialographic techniques, and grain sizes were determined by the circle intercept method. In addition, a few samples were examined with aid of a transmission electron microscope (TEM). Specimens were cut perpendicular to the testing (extrusion) direction and then mechanically ground on 600 grit SiC paper to ~ 100 μm thick. These were electrochemically thinned at 40 V and 10 mA using a 10% perchloric acid–ethanol solution at −10° C prior to viewing in the TEM.

3. Results

3.1. Materials

Both the direct extrusion and compaction followed by extrusion techniques yielded fully dense NiAl intermetallic compounds. Materialographic examination of transverse and longitudinal sections revealed that

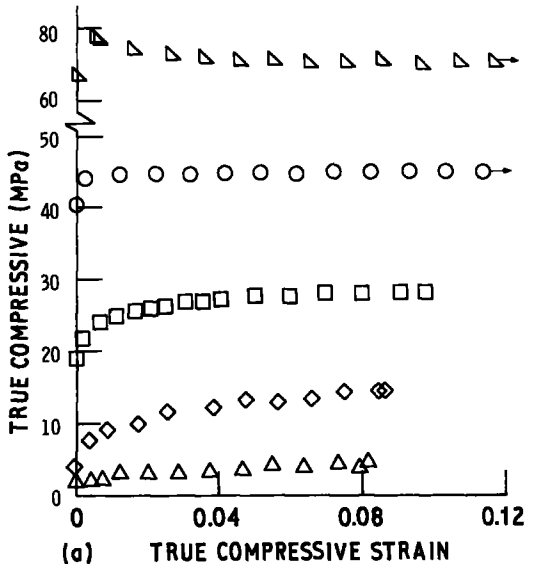

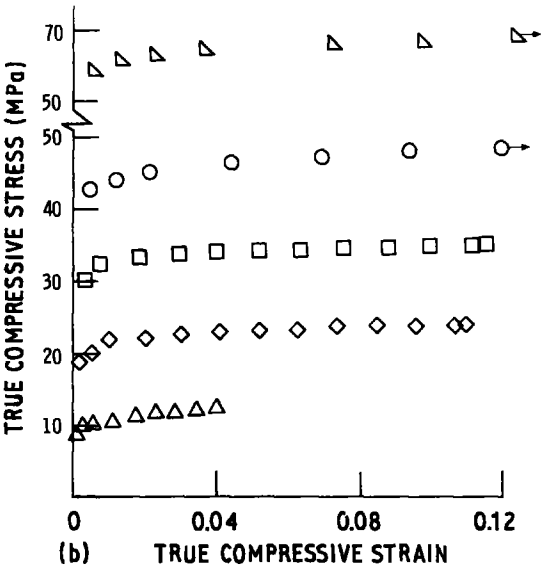

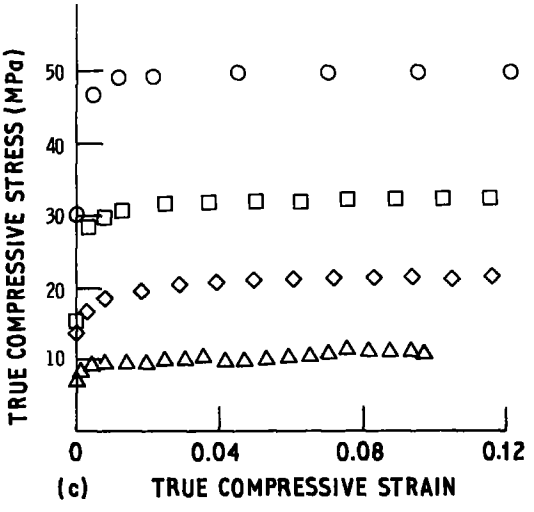

Figure 1 Typical true compressive stress–strain diagrams at 1300 K as a function of approximate strain rate and composition. (a) Ni–52.7 Al. Strain rates (sec^{-1}): (◺) 1.85×10^{-3}, (○) 1.85×10^{-4}, (□) 1.7×10^{-5}, (◇) 1.7×10^{-6}, (△) 1.7×10^{-7}. (b) Ni–49.2 Al. Strain rates (sec^{-1}): (◺) 2.4×10^{-3}, (○) 2.4×10^{-4}, (□) 2.25×10^{-5}, (◇) 2.2×10^{-6}, (△) 2.15×10^{-7}. (c) Ni–43.9 Al. Strain rates (sec^{-1}): (○) 2.4×10^{-4}, (□) 2.25×10^{-5}, (◇) 2.25×10^{-6}, (△) 2.2×10^{-7}.

each material had recrystallized during extrusion to an approximately equiaxed grain size with some interspersed oxides. These are probably the result of powder processing and comprise about 0.4 vol % as estimated by quantative image analysis of polished surfaces. X-ray techniques for preferred orientation indicated that the NiAl materials were not textured.

Electron microprobe analysis of longitudinal sections indicated that the chemistry of the as-extruded material was not completely homogeneous with wide (up to 60 μm) aluminium-rich or aluminium-deficient regions being occasionally found. A similar examination, however, of a specimen which had been compression tested at 1200 K and a strain rate of $\sim 2 \times 10^{-5} sec^{-1}$ for about 6×10^3 sec (lowest test temperature, fastest test conditions for a blended product) revealed that the chemical inhomogeneities had been almost completely eliminated.

3.2. Mechanical properties

3.2.1. Stress–strain

Several true compressive stress–strain diagrams illustrating typical behaviour as functions of strain rate and composition are given in Fig. 1 for tests conducted at 1300 K. Three types of curves were observed; the most common, by far, involved a rapidly increasing stress during the first ~2% deformation followed by further straining at a constant or very slowly increasing stress. Occasionally, yielding followed by flow at a somewhat lower (within a few MPa), approximately constant, stress was seen for the fastest tests (Fig. 1a), and for the slowest tests at the higher temperatures examples of continuous work hardening to 5% or more strain followed by flow at a nearly constant stress, were found. Comparison of the stress–strain diagrams reveals that the strength for the hyperstoichiometric aluminium intermetallic compound (Fig. 1a) is less than that of either the 49.3 or 43.9 aluminium materials (Figs 1b and c). However, the strengths of the latter two alloys are approximately equal.

3.2.2. Stress–strain rate

Flow stress, σ, and strain rate, $\dot{\varepsilon}$, were taken from the stress–strain curves to reflect the maximum strength measured in this study where σ, $\dot{\varepsilon}$ are (1) average values for the nominally constant flow conditions, (2) values from the yield points when yielding occurred, or (3) values at ~10% strain when continuous work hardening took place. It is believed that the latter two choices of σ and $\dot{\varepsilon}$ are reasonable. When yielding was observed, there was little difference between the stress at the yield point and that required for continued deformation (Fig. 1). In the case of continuous work hardening type stress–strain behaviour, the rate of work hardening had diminished to the point that continued straining beyond 10% strain would only require a slightly higher stress (Fig. 1).

Typical compressive true stress–true strain rates

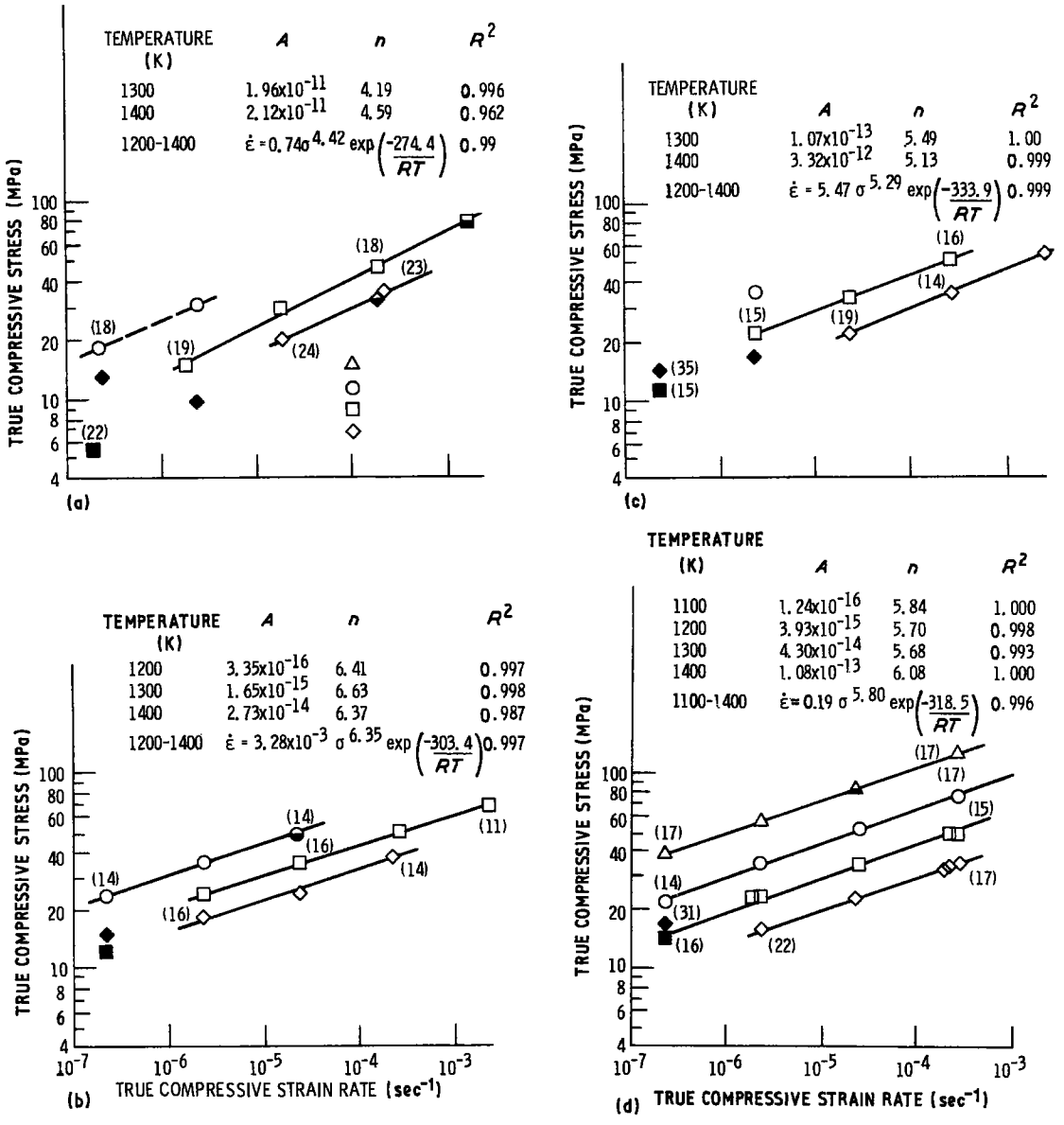

Figure 2 True compressive flow stress–strain rate curves as a function of temperature and composition. (a) Ni–52.7 Al, (b) Ni–49.2 Al, (c) Ni–43.9 Al and (d) Ni–48.25 Al. Filled symbols denote data taken from work hardening type stress–strain curves, half filled symbols are data from stress–strain curves which had yield points, and open symbols denote data from stress–strain diagrams which exhibited flow at an approximately constant stress. Data in parentheses denote grain size (μm) after testing. Temperatures (K): (△) 1100, (○) 1200, (□) 1300, (◇) 1400.

as a function of composition and temperature are presented in Fig. 2 with the data taken from stress–strain curves showing (1) yield points by half filled symbols, (2) extended work hardening by filled symbols, and (3) continued flow at an approximately constand stress by open symbols. Figs 2a to c illustrate behaviour of materials extruded using 51 mm steel cans at 1420 K while Fig. 2d shows data for an alloy initially hot compacted and then extruded at 1505 K out of 76 mm cans. For documentation flow stress–strain rate data for the remaining six alloys are given in the Appendix.

Basically the flow stress–strain rate data for NiAl can be well described by power law creep

$$\dot{\varepsilon} = A\sigma^n \qquad (1)$$

where A is a constant, and n is in the stress exponent for creep. Values of A and n and the coefficient of determination, R^2, were calculated by linear regression techniques and are given in Fig. 2 and the Appendix where the solid lines denote the valid regime for each fit. While all data could be fitted to Equation 1 for 1100 and 1200 K tests, at higher temperatures the regression analyses were, in general, only reasonable for strain rates greater than $10^{-6}\,\mathrm{sec}^{-1}$. Two types of deviations from power law behaviour were seen with actual flow stresses being less than (1300 K, $\dot{\varepsilon} \sim 2 \times 10^{-7}$ in Figs 2a, b and c) or greater than (1400 K, $\dot{\varepsilon} \sim 2 \times 10^{-7}\,\mathrm{sec}^{-1}$ in Fig. 2) the extrapolated values. In all cases these deviations could be connected to stress–strain diagrams which exhibited extended work hardening to 5% or more strain.

The flow stress–strain rate–temperature data for each material was also fitted to the usual temperature compensated-power law creep model

$$\dot{\varepsilon} = B\sigma^n \exp(-Q/RT) \qquad (2)$$

where B is a constant, Q is the activation energy for creep ($\mathrm{kJ\,mol}^{-1}$), and RT have their usual meaning. The results of linear regression fits to this equation are

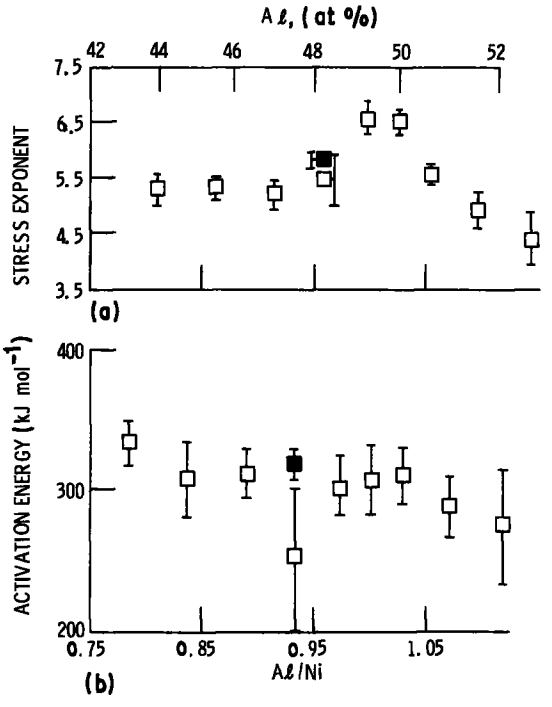

Figure 3 (a) Stress exponent and (b) activation energy for creep in NiAl as a function of composition. Filled symbol designates the 48.25 Al material produced from prealloyed powder.

also presented in Fig. 2 and the Appendix, and the stress exponents and activation energies along with 90% confidence limits are shown as a function of composition in Fig. 3. These data indicate that n peaks at ~ 6.5 for slightly aluminium defficient compositions, is approximately constant at 5.3 over a wide range in hypostoichiometric compositions ($0.78 \leqslant$ Al/Ni $\leqslant 0.93$), and continuously decreases with increasing aluminium level for Al/Ni > 1.00. The activation energy for creep appears to be constant and equal to $310\,\mathrm{kJ\,mol^{-1}}$ over most of the composition range except for the extreme hypo- and hyperstoichiometric chemistries where Q could slightly increase with decreasing aluminium level and decrease with increasing aluminium content.

Although stress exponents vary with composition (Fig. 3a) and the activation energy could be slightly dependent of aluminium content, comparison of all the flow stress–strain rate data (Fig. 2 and the Appendix) reveals that the creep strength of materials with Al/Ni $\leqslant 1.03$ are essentially equal. The more aluminium rich alloys, on the other hand, tend to be weaker. In addition, comparison of the mechanical properties of the two 48.25 Al alloys permits an evaluation of the major difference between the two processing techniques: prealloyed powder compared with powder blending. Use of a dummy variable and linear regression techniques in conjuction with Equations 1 and 2 indicate that there is no statistical difference (95% level) between the σ–$\dot{\varepsilon}$ behaviour of the 48.25 Al materials. Therefore blending of two lots of prealloyed NiAl powder to produce intermediate compositions for elevated temperature mechanical property testing seems to be valid alloying procedure.

3.3. Post test microstructure

Typical longitudinal microstructures for several tested intermetallics are presented in Fig. 4. A 25 HNO_3, 25 acetic acid, 50 H_2O and 1 HF (parts by volume) etchant produced excellent results on hyperstoichiometric alloys (Fig. 4a); unfortunately this mixture would not attack stoichiometric or lesser aluminium levels, and the usual solution of 33 HCl, 33 HNO_3, and 33 acetic acid was utilized for the remaining materials (Fig. 4b). Grain sizes measured from the polished and etched specimens are shown in parentheses above the appropriate data points in Fig. 2 and the Appendix.

Several observations can be made about the general microstructure of compression-tested NiAl. No evidence of grain-boundary cracking was seen, and preferred oxidation along grain boundaries did not take place; however, selective aluminium diffusion to the exposed surfaces apparently does occur based on the inability of the 25 HNO_3, 25 acetic acid, 50 H_2O, 1 HF mixture to reveal the grain structure near the edge (Fig. 4a). The appearance of the as-extruded grain structure basically remained unchanged by elevated temperature testing; although exposure to fast deformation–low temperature conditions tended to produce waviness in the grain boundaries (Fig. 4b).

Comparison of the as-extruded grain sizes (Table I) to those of tested materials (Fig. 2 and the Appendix)

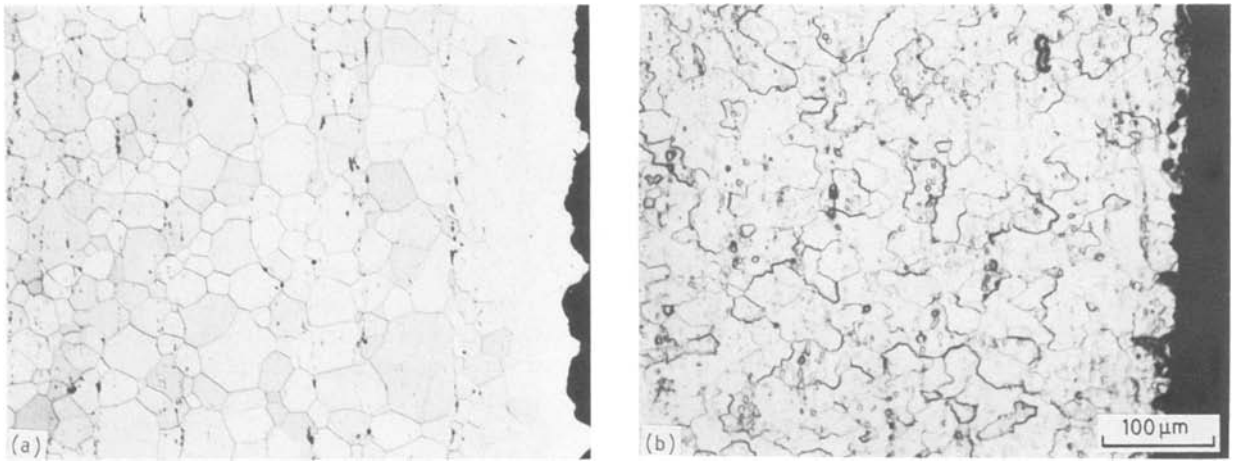

Figure 4 Typical post test microstructures for NiAl. (a) Ni–52.7 Al tested at 1400 K and $\dot{\varepsilon} \sim 1.7 \times 10^{-5}\,\mathrm{sec^{-1}}$ to 9.6% strain, (b) Ni–48.25 Al tested at 1100 K and $\dot{\varepsilon} \sim 2.35 \times 10^{-4}\,\mathrm{sec^{-1}}$ to 23.1% strain.

TABLE II Estimated flow stresses necessary to produce strain rates of 1.33×10^{-5} and 1.33×10^{-6} sec^{-1} in NiAl

Composition		Flow stress at (MPa)				Reference
Al	Al/Ni	1200 K		1300 K		
		1.33×10^{-5} sec^{-1}*	1.33×10^{-6} sec^{-1}	1.33×10^{-5} sec^{-1}	1.33×10^{-6} sec^{-1}	
54	1.17	40	20	21	10	[8]
54	1.17	24	–	13	–	[5]
52.7	1.12	42	26	24.5	14	This study
52	1.08	46	27	35	18	[8]
50.4	1.02	31	–	17.5	–	[5]
50.25	1.01	61.5	28.5	35.5	16	[9]
50	1.00	52	33	33	20	[8]
49.91	1.00	–	–	30	20.5	This study
49.2	0.97	45	31	31	22	This study
45	0.82	73	40	39	22	[8]
44	0.79	38	–	19	–	[5]
43.9	0.79	–	–	29	19	This study

*Strain rates.

indicates that little, if any, grain growth occurred during deformation at 1300 K or lower temperatures. Similarly grain growth was not evident at 1400 K for strain rates greater than $2 \times 10^{-6} sec^{-1}$; however, 1400 K – $\dot{\varepsilon} \sim 2 \times 10^{-7} sec^{-1}$ testing generally resulted in some increase in average grain diameter (Fig. 2 and the Appendix).

4. Discussion

In general, the present results compare favourably with those in the literature in terms of creep strength as can be seen in Table II. The data are presented in three groups representing hyper-, near equiatomic, and hypo-aluminium compositions and were obtained by fitting Equation 2 to given $\dot{\varepsilon}$–σ–T values and back calculating for $\dot{\varepsilon} = 1.33 \times 10^{-5}$ and $\dot{\varepsilon} = 1.33 \times 10^{-6} sec^{-1}$ conditions. The strength of Vandervoort *et al.*'s materials [5] is less than that of the other intermetallic materials. On the other hand, the behaviour of Yang and Dodd's alloys [8] and that of this study are in basic agreement. The most interesting comparison of data is that for the near stoichiometric materials where nearly equivalent strength is found in three widely divergent forms: i.e. the polycrystalline 450 μm grain size alloy of Yang and Dodd, the ~ 15 μm diameter polycrystals of the present work, and the near centre of the stereographic triangle oriented NiAl single crystals of Hocking *et al.* [9]. Discounting the results of Vandervoort *et al.*, agreement among the above three studies indicates a lack of dependency on grain size for grain diameters greater than 15 μm.

In addition to actual creep strengths, the stress exponents and activation energies determined in this study can be compared to those in the literature. These data are shown in Fig. 5 and include both single crystal [10, 15] and polycrystalline [5, 8, 16] forms. Except for Vandervoort *et al.*'s low value near stoichiometry, the concentration dependency of the stress exponents from the other investigations is in general agreement with the current results; however, an absolute difference of 1 to 2 units exists between the two sets of data.

With regard to activation energy (Fig. 5b) all data cluster between 260 and 340 kJ mol^{-1}; however, the present results reveal that the concentration dependency of Q is much smoother than previously thought [8]. In fact, the present almost concentration-independent behaviour of the activation energy for creep is in sharp contrast to the existing diffusion data. For example, the tracer diffusion coefficients of ^{63}Ni [17], ^{60}Co [18] and ^{114}In [19] in NiAl generally show large discontinuties in the tracer activation energy–concentration behaviour. Hancock and McDonnell [17], for instance, report an increase in energy from ~ 190 kJ mol^{-1} at 49 Al to ~ 310 kJ mol^{-1} at 50 Al. In addition, Shankar and Siegle [20] have found that the activation energy for interdiffusion varies greatly with concentration where it peaks at ~ 250 kJ mol^{-1} for 45 Al and parabolically decreases to ~ 140 kJ mol^{-1} at 53 Al.

While the present compositional dependency of n and Q is more continuous than past determinations,

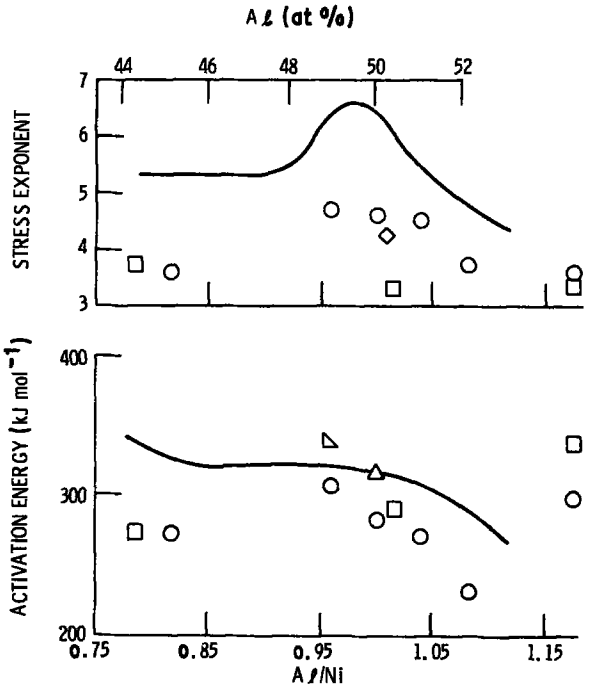

Figure 5 Values of (a) the stress exponent and (b) activation energy for creep in NiAl from previous investigations as a function of composition. (□) [5], (○) [8], (◇) [10], (△) [15], (▷) [16], (——) present work.

the observation of nearly equivalent creep strength in NiAl materials with Al/Ni $\leqslant$ 1.03 is bothersome. Such a result argues that only a single deformation mechanism exists with a unique, concentration-independent stress exponent and activation energy, and that the data in Fig. 3 are simply due to the linear regression technique and experimental error. This concept is supported by the apparently unsystematic variation of the pre-exponential constant in Equation 2 with composition (Fig. 2 and the Appendix). To examine the possibility of single valued n and Equation 2 where

$$\dot{\varepsilon} = 0.16\sigma^{5.75} \exp(-314.2/RT) \quad (3)$$

with $R^2 = 0.99$, and the standard deviation of n and Q are 0.08 and 5.1 kJ mol^{-1}, respectively. Statistical testing of Equation 3 against other models, which included a concentration-dependent pre-exponential term, grain size, and dummy variable for composition, revealed that all flow stress–strain rate data were adequately described by Equation 3. Hence it is probable that creep in NiAl is independent of concentration for Al/Ni < 1.03. This is in agreement with the work of Lasalmonie [21] who concluded that the deformation mechanism in nickel-rich aluminides was not a function of composition between 900 and 1200 K.

Comparison of the data which can be described by Equations 1 and 2 to that in the literature that creep strength of NiAl is independent of grain size. However, this is probably not always true as examples of creep strength above and below predicted values have been noted under certain test conditions (Fig. 2a for 1400 and 1300 K, $\dot{\varepsilon} \sim 2 \times 10^{-7}$ sec^{-1}, for instance). It is believed that these deviations can be explained on the basis of a subgrain concept of creep and the transition from normal climb/glide dislocation mechanisms to diffusional creep. These two models lead to deformation conditions where grain size can control the straining rate.

Subgrains unquestionably form in NiAl for many direct observations of subboundaries [4, 7–11, 22] and indirect evidence through wavy grain boundaries (Fig. 4b) exist. According to Sherby *et al.* [23] the subgrain size, λ, can have a profound effect on steady state creep rate

$$\dot{\varepsilon} \propto (\lambda/\boldsymbol{b})^3 (\sigma/E)^8 D_{\text{eff}} \quad (4)$$

where $\boldsymbol{b}$ is the magnitude of the Burgers vector, E is the dynamic elastic modulus, and D_{eff} is an effective diffusion coefficient which includes contributions due to lattice diffusion and dislocation pipe diffusion.

Because

$$\lambda \propto (E/\sigma) \quad (5)$$

the influence of subgrain size is, in general, not directly seen, and

$$\dot{\varepsilon} \propto (\sigma/E)^5 D_{\text{eff}} \quad (6a)$$

or when E varies only slightly with temperature

$$\dot{\varepsilon} \propto \sigma^5 D_{\text{eff}} \quad (6b)$$

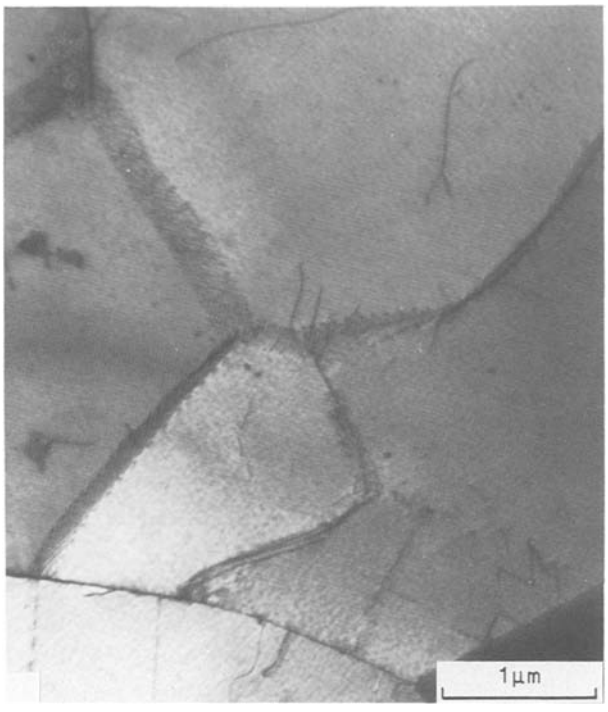

Figure 6 Transmission electron photomicrograph of subgrain boundaries found in Ni–49.2 Al tested at 1200 K and $\dot{\varepsilon} \sim 2.3 \times 10^{-6}$ sec^{-1} to 14.1% strain.

type behaviour is found. The existence of subgrains in NiAl and the similarity in Equation 6b and current descriptions (Equation 3) suggest that creep in this intermetallic material is basically controlled by the subgrain size.

The transition from Equation 4 to Equation 6 is only possible when the subgrain size is inversely proportional to stress (Equation 5). If a small grain size d, is maintained in NiAl during creep, then Equation 5 will no longer be obeyed under low stress conditions, because the subgrain size cannot exceed the grain size. Hence Equation 4 would become

$$\dot{\varepsilon} \propto (d/\boldsymbol{b})^3 (\sigma/E)^8 D_{\text{eff}} \quad (7)$$

When the subgrain size is restricted to the grain size, a material under some stress σ would creep at a lesser rate than that predicted by Equation 4, since d is smaller than the subgrain size which would normally be established. Similarly for the constant velocity test conditions imposed in this work, creep via Equation 7 would require a higher flow stress than that under Equations 3 or 6.

The above model is based on the formation of subboundaries during creep; basically it contends that in fine grain size NiAl lower temperatures or faster strain rates would result in subgrains while under higher temperature or slower strain rate conditions, subboundaries should not be present. To examine the validity of this concept, thin foils were taken from selected specimens of Ni–49.2 Al and studied by TEM. No subboundaries were seen in the as-extruded aluminide; however, subgrains are found in specimens tested at faster strain rates for all test temperatures, and an example is presented in Fig. 6. While subgrains were noted after fast straining, examination of the slowest strain rate ($\dot{\varepsilon} \sim 2 \times 10^{-7}$ sec^{-1}) specimens

indicated that the 1300 and 1400 K samples were devoid of subboundaries, but subgrains were established during 1200 K testing. These microstructural observations are in agreement with the proposed model linking the formation of subgrains to the test conditions and grain size.

Although subgrain strengthening appears to be a major factor, due to the high test temperatures and small grain size of the current materials, diffusional creep mechanisms could also be expected to contribute to the observed deformation rate. For example the theoretical Nabarro-Herring creep rate for a 20 μm grain size material tested at 1300 K and 10 MPa would be about $10^{-6}\,sec^{-1}$ based on Hancock *et al.*'s tracer coefficients [17]. Since the low strength deviation from Equations 1 and 2 generally occurred at 1300 K, $\dot{\varepsilon} \sim 2 \times 10^{-7}\,sec^{-1}$ and 1400 K, $\dot{\varepsilon} \sim 2 \times 10^{-6}\,sec^{-1}$ conditions (Fig. 3 and the Appendix), it is conceivable that diffusional creep is making a significant contribution to deformation in these high temperature, slow plastic flow regimes, and a lower creep strength results.

Apparently under the higher temperature–lower strain rate test conditions both dislocation creep

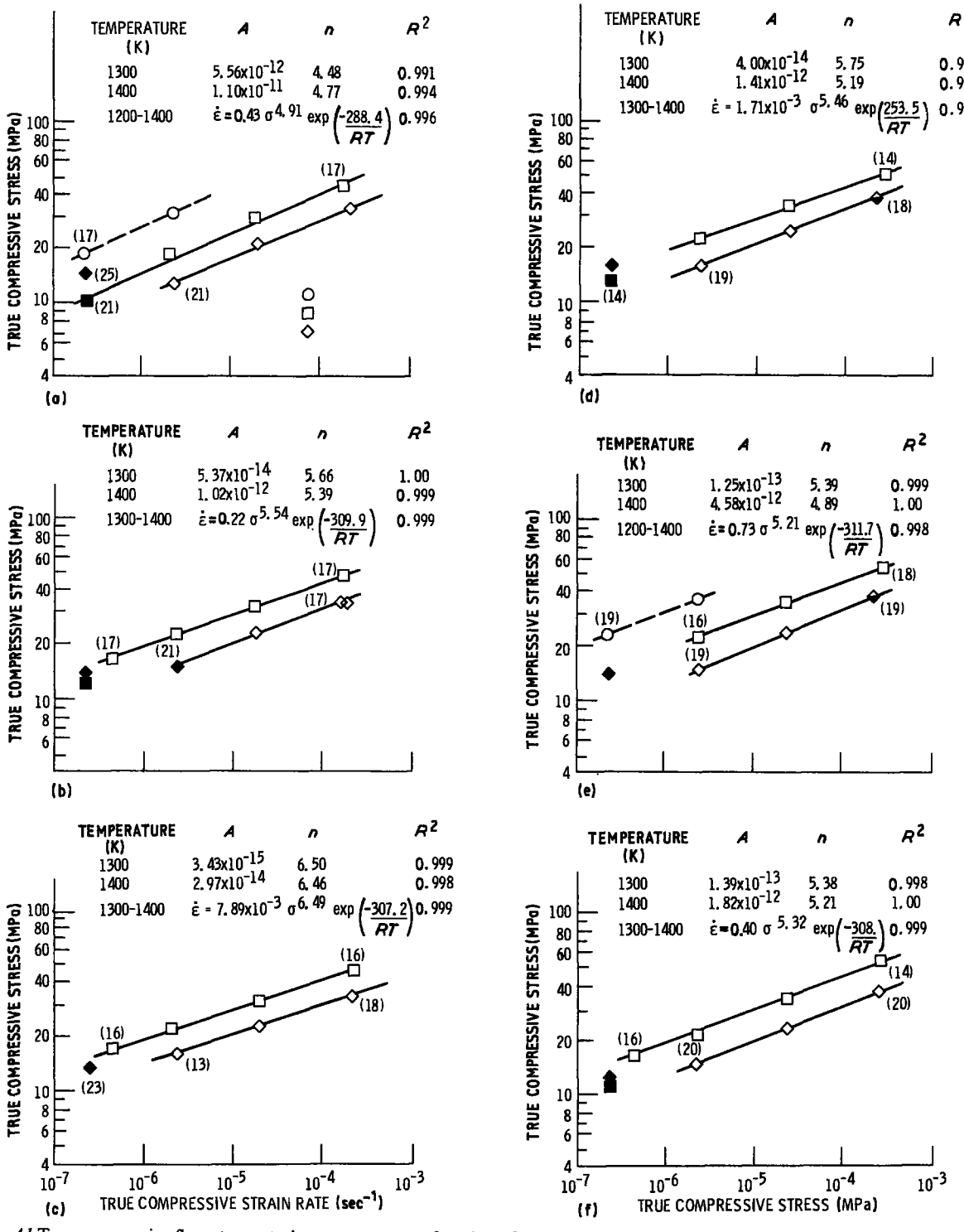

Figure A1 True compressive flow stress–strain rate curves as a function of temperature and composition. (a) Ni–51.6 Al, (b) Ni–50.6 Al, (c) Ni–49.91 Al, (d) Ni–48.25 Al, (e) Ni–47 Al and (f) Ni–45.5 Al. Filled symbols denote data taken from work hardening type stress–strain curves, half filled symbols are data from stress–strain curves which had yield points, and open symbols denote data from stress–strain diagrams which exhibited flow at an approximately constant stress. Data in parentheses denote grain size (μm) after testing. Temperatures (K): (○) 1200, (□) 1300, (◇) 1400.

involving formation of subgrains and diffusional creep can simultaneously occur in small grain size NiAl. These mechanisms are influenced by changes in grain size where an increase in grain diameter would decrease the diffusional creep but increase the grain size controlled rate (Equation 7). Because the relative contribution of each mechanism to the overall creep rate is unknown and would be affected by temperature, stress and grain size, odd behaviour, such as the flow stress for 1400 K being greater than that for 1300 K, could result.

Finally it should be noted that a difference in creep behaviour exists between metals/alloys and B2 intermetallic compounds such as CoAl [14], FeAl [13, 24] and NiAl. In these aluminides maintenance of a fine grain size either has no effect (CoAl and NiAl) or even increases (FeAl) the creep strength up to high fractions of the melting point (~ 0.7) while in metallic systems a small, polycrystalline grain size leads to drastic loss in strength at temperatures above approximately half the melting point.

5. Summary of results

Compression testing of a series of small grain size, polycrystalline NiAl materials between 1200 and 1400 K indicates that:

1. creep strength is independent of composition for Al/Ni $\leqslant$ 1.03, and deformation can be adequately described by a single stress exponent and activation energy;

2. for lower temperature, higher strain rate conditions, creep seems to be controlled by the formation of subgrains;

3. based on data in the literature, creep at fast strain rates and lower temperatures is independent of grain size;

4. for slower strain rates and higher temperatures creep can be affected by grain size;

5. powder blending techniques to produce intermediate compositions appears to be valid alloying procedure.

Appendix

For documentation, compressive flow stress–strain rate diagrams for the remaining six materials tested in this study are presented in Fig. A1.

References

1. E. M. GRALA, Investigations of NiAl and Ni_3Al, in "Mechanical Properties of Intermetallic Compounds", edited by J. H. Westbrook (Wiley, New York, 1960) pp. 358–404.
2. E. P. LAUTENSCHLAGER, D. A. KIEWIT and J. O. BRITTAIN, *Trans. Met. Soc. AIME* **233** (1965) 1297.
3. A. G. ROZNER and R. J. WASILEWSKI, *J. Inst. Metals* **94** (1966) 169.
4. A. BALL and R. E. SMALLMAN, *Acta Metall.* **14** (1966) 1349.
5. R. R. VANDERVOORT, A. K. MUKHERJEE and J. E. DORN, *Trans. ASM* **59** (1966) 930.
6. R. T. PASCOE and C. W. A. NEWEY, *Met. Sci. J.* **2** (1968) 138.
7. P. R. STRUTT, R. A. DODD and G. M. ROWE, "Creep in Stoichiometric NiAl", Second International Conference on the Strength of Metals and Alloys, Vol. III, (ASM, Metals Park, Ohio, 1971) pp. 1057–61.
8. W. J. YANG and R. A. DODD, *Met. Sci. J.* **7** (1973) 41.
9. L. A. HOCKING, P. R. STRUTT and R. A. DODD, *J. Inst. Met.* **99** (1971) 98.
10. J. BEVK, R. A. DODD and P. R. STRUTT, *Met. Trans.* **4** (1973) 159.
11. H. L. FRASER, R. E. SMALLMAN and M. H. LORETTO, *Phil. Mag.* **28** (1973) 651.
12. E. M. SCHULSON and D. R. BARKER, *Scripta Metall.* **17** (1983) 519.
13. J. D. WHITTENBERGER, *Mat. Sci. Eng.* **57** (1983) 77.
14. *Idem, ibid.* **73** (1985) 8796.
15. W. R. KANNE Jr, P. R. STRUTT and F. A. DODD, *Trans. AIME* **245** (1969) 1259.
16. R. T. PASCOE and C. W. A. NEWEY, *Met. Sci. J.* **5** (1971) 50.
17. G. F. HANCOCK and B. R. McDONNELL, *Phys. Status Solidi (a)* **4** (1971) 143.
18. A. E. BERKOWITZ, F. E. JAUMOT Jr and F. C. NIX, *Phys. Rev.* **95** (1954) 1185.
19. A. LUTZE-BIRK and H. JACOBI, *Scripta Metall.* **9** (1975) 761.
20. S. SHANKAR and L. L. SIEGLE, *Met. Trans. A* **9A** (1978) 1467.
21. A. LASALMONIE, *J. Mater. Sci.* **17** (1982) 2419.
22. E. P. LAUTENSCHALAGER, T. C. TISONE and J. O. BRITTAIN, *Phys. Status Solidi* **20** (1967) 443.
23. O. D. SHERBY, R. H. KLUNDT and A. K. MILLER, *Met. Trans. A* **8A** (1977) 843.
24. J. D. WHITTENBERGER, *Mat. Sci. Eng.* **77** (1986) 103.

Received 23 December 1985
and accepted 6 May 1986